

Towards a statistical theory of transport by strongly-interacting lattice fermions

Subroto Mukerjee,^{*} Vadim Oganesyan,[†] and David Huse[‡]
Department of Physics, Princeton University, Princeton NJ 08544
(Dated: October 23, 2018)

We present a study of electric transport at high temperature in a model of strongly interacting spinless fermions without disorder. We use exact diagonalization to study the statistics of the energy eigenvalues, eigenstates, and the matrix elements of the current. These suggest that our nonrandom Hamiltonian behaves like a member of a certain ensemble of Gaussian random matrices. We calculate the conductivity $\sigma(\omega)$ and examine its behavior, both in finite size samples and as extrapolated to the thermodynamic limit. We find that $\sigma(\omega)$ has a prominent non-divergent singularity at $\omega = 0$ reflecting a power-law long-time tail in the current autocorrelation function that arises from nonlinear couplings between the long-wavelength diffusive modes of the energy and particle number.

PACS numbers: Valid PACS appear here

I. INTRODUCTION

The subject of transport in strongly-correlated electron systems is of considerable current interest, motivated, for example, by recent experiments on cuprate and cobaltate materials measuring electrical and thermal transport properties [1, 2]. Traditionally, much of the work has focused on the behavior of quantum systems at low temperatures [3], where transport properties can be used to characterize a material's ground state. Under these conditions, the excitations responsible for transport are often dilute and weakly interacting ("quasiparticles"), thus allowing for a straightforward description of transport, e.g. using the Boltzmann (kinetic) equation formalism [4]. Interestingly, in the opposite extreme, when temperature is high and no well defined elementary excitations exist, transport properties remain nontrivial and difficult to calculate and understand [5]. Additionally, what makes studying this regime worthwhile is the fact that sometimes interesting phenomena take place over a broad temperature range, extending up to temperatures so high that direct interpretations in terms of low temperature universal properties (either conventional or exotic) can be questioned, thus leaving the high temperature regime addressed in this work as a promising starting point of analysis. Although we attempt no detailed comparisons with experiments here, it may be of interest to note that the optical conductivity we find is very broad, extending over frequencies of order the bare bandwidth, with DC resistivity growing linearly with temperature. These features are remarkably reminiscent of what is often observed in the normal state of correlated materials as diverse as organic salts, CDW systems, C_{60} and even high temperature superconductors. However, further work is necessary to elucidate possible implications of our high temperature approach to any specific material.

In this paper, we study the conductivity, σ , as a function of frequency ω and temperature T . For a finite quantum system with a discrete spectrum, the real part of the conductivity at nonzero frequency is given by the Kubo formula:

$$\sigma(\omega, T) = \pi \frac{1 - e^{-\beta\hbar\omega}}{\omega Z} \sum_{n,m} e^{-\beta E_n} |J_{nm}|^2 \delta(E_n - E_m - \hbar\omega), \quad (1)$$

where n and m are eigenstates of the Hamiltonian, E_n and E_m are the corresponding energy eigenvalues, J_{nm} is the matrix element of the total current operator between these two states, $\beta = 1/k_B T$ and Z is the partition function. Note that we do not include any "external" dissipative bath; what we are studying is the absorption of energy from an infinitesimal applied AC electric field by transitions between eigenstates of the Hamiltonian.

One thing we investigate here is how the above singular expression for the conductivity converges to a continuous function in the thermodynamic limit. It is a sum of delta-functions, one for each pair of energy eigenstates that are connected by the current operator. The number of eigenstates scales exponentially in the number of degrees of freedom in the system $\sim e^{sL^d}$, where L is system's linear extent and s is the entropy density, with average level spacing $\Delta \sim e^{-sL^d}$. For a generic non-integrable Hamiltonian there are only a few good quantum numbers. These include the total number of particles, the Bloch (lattice) momentum for systems with discrete translational invariance, and in some models of interest the total spin. All pairs of states with the same quantum numbers generically contribute a delta-function to the conductivity, and so the total number of terms in the sum scales as $\sim e^{2sL^d}$. Thus the number of delta-functions in $\sigma(\omega)$ grows very rapidly both with increasing system size and with increasing temperature (and thus s), and away from zero frequency a good approximation to the thermodynamic limit is rapidly approached with only very fine binning or other smoothing of the delta-functions. However, there are significant and interesting finite size effects present near zero frequency, and elucidating them is one of the main topics of this paper.

^{*}Electronic address: mukerjee@princeton.edu

[†]Electronic address: voganesy@princeton.edu

[‡]Electronic address: huse@princeton.edu

For models where a finite-sized system has a bounded spectrum and a finite-dimensional Hilbert space, such as the one-band model of interacting lattice fermions that we will study here as our example Hamiltonian, the above expression simplifies in the high temperature limit to

$$k_B T \sigma(\omega) \approx \frac{\pi \hbar}{Z} \sum_{n,m} |J_{nm}|^2 \delta(E_n - E_m - \hbar\omega). \quad (2)$$

We will mostly focus on this limiting behavior of the conductivity, since it is already nontrivial. However, all of the features we will discuss appear to apply at finite temperatures as well. One basic noteworthy feature of this high T limit is that the resistivity is proportional to the temperature.

Such a simple statistical characterization of the conductivity breaks down at low temperatures and frequencies. At low temperatures both thermodynamics and dynamics are dominated by comparatively few transitions from low energy states residing in the tail of the Hamiltonian's full spectrum, and their properties may depend on specific details of the system and its ground state. The low frequency part of the high temperature conductivity, on the other hand, shows various finite size effects that can be understood based on rather general considerations:

i) Level repulsion reduces the number of pairs of states with a very small energy difference, producing an underestimate of the macroscopic low-frequency conductivity (in fact, σ vanishes as $\omega \rightarrow 0$);

ii) If the above formula (1) for the conductivity of a finite system is applied precisely at $\omega = 0$, we find a delta function due to the current's diagonal matrix elements J_{nn} . For integrable Hamiltonians this delta-function has a nonzero weight in the thermodynamic limit, hence the macroscopic DC conductivity appears to be infinite at all temperatures. In weakly non-integrable systems this delta function is weakly broadened, it is the celebrated Drude peak. In our case, and in non-integrable systems more generally, the weight of this precisely elastic delta-function in the conductivity scales exponentially to zero with increasing system size, as discussed in Section IV below.

iii) Finally, in the infinite system there is a non-divergent zero-frequency singularity of the form $\sigma(\omega = 0) - \sigma(\omega) \sim \omega^{d/2}$ due to nonlinear couplings between the long-wavelength diffusive energy and particle density modes. This singularity is rounded by finite-size effects.

We discuss and disentangle all of these effects (as well as demonstrate the general validity of considerations away from $\omega = 0$) using a simple one dimensional model as a case study. While some of the results are special to the particular model, e.g. the dependence of the low frequency non-analyticity on dimension and range of interactions, the overall picture that emerges is clear and robust against variations in parameters, and most features are not special to one dimension. It also appears to apply at all temperatures in the disordered phase provided

$\beta\omega \ll 1$. In Section II we present the Hamiltonian under study as well as the numerical procedures employed to solve the problem exactly for finite sizes. In Section III we use the exact numerical results to study statistical properties of the spectrum and the eigenstates, including the matrix elements of the current operator. The conductivity is computed and discussed in Section IV, and its diffusion-induced non-analyticity is analyzed in Section V. Finally, we conclude with a brief overview and list of open questions.

II. $t - t' - V$ MODEL AND EXACT DIAGONALIZATION

Although much of what we find is rather generic to non-integrable quantum many-body solid-state systems, the specific model we consider here is a one dimensional chain of spinless fermions with a single tight-binding orbital at each site. The Hamiltonian is

$$H = -t \sum_j c_j^\dagger c_{j+1} - t' \sum_j c_j^\dagger c_{j+2} + \text{h.c.} + V \sum_j n_j n_{j+1}, \quad (3)$$

where c_j^\dagger , c_j and $n_j = c_j^\dagger c_j$ are fermion creation, annihilation and density operators, respectively. This is one of the simplest non-integrable (quantum chaotic) many-particle models. For spinless lattice fermions the size of the Hilbert space is small, with only 2 states per site, and thus 2^L states for a chain of length L sites. We have a short-range (nearest-neighbor) interaction V (spinless lattice fermions cannot have an on-site interaction). The second-neighbor hopping t' makes the Hamiltonian non-integrable and also breaks particle-hole symmetry. This system's good quantum numbers (conserved quantities in addition to the energy) are total particle number and total crystal momentum. As written above, with the periodic boundary conditions that we use, it also has parity symmetry. We have chosen to break parity with an irrational phase twist at the boundary (equivalent to threading a fraction of a magnetic flux quantum through the loop). This minimizes the number of distinct symmetry sectors to those labeled by the two good quantum numbers. We have also looked at the model where the second-neighbor hopping is replaced by a second-neighbor interaction; this latter model is equivalent to that studied by Rabson, *et al.* [6]. We chose to focus instead on our model because we did not want particle-hole symmetry. However, the results we present are generally independent of the presence or absence of any of these symmetries other than conserved particle number. Similar models have been used in earlier studies of charge, heat and/or spin transport and the crossover from integrability to non-integrability [5, 6].

For this model the operator for the total particle current is

$$J = \frac{it}{\hbar} \sum_j c_j^\dagger c_{j+1} + \frac{2it'}{\hbar} t' \sum_j c_j^\dagger c_{j+2} + \text{h.c.} \quad (4)$$

We have also looked at heat transport and thermopower, with similar preliminary results; this work will be reported later. We work for convenience at half filling, and average over the different total crystal momentum sectors. It appears, as we expect, that the behavior is statistically the same in each such momentum sector, and that there is nothing special about half filling for the regimes and properties we examine. We specifically take $t = t' = 1$ and $V = 2$, so the interaction is roughly equal to the single-particle bandwidth, and thus strong. All energies are measured in units of $t = t' = 1$, frequencies in units of $t/\hbar = 1$, and lengths in units of the lattice spacing.

We use a Householder diagonalization routine to exactly diagonalize the Hamiltonian within each momentum sector (typically 16 or 18 sites, with 8 or 9 particles, respectively). For convenience, we choose to work in the basis of single-particle momentum eigenstates. These states are also eigenstates of the total current operator, so this is one of the two “natural” bases for this problem. The other natural basis is less simple; it is that of the eigenstates of the other operator that enters in determining the conductivity, namely the Hamiltonian itself.

III. STATISTICS OF THE SPECTRUM, EIGENSTATES AND CURRENT MATRIX ELEMENTS

One of the common measures used to characterize the spectrum of a non-integrable quantum Hamiltonian is the (Wigner-Dyson) distribution of level spacings. Our Hamiltonian is a real matrix (this is true in our basis of single-particle momentum eigenstates even with a magnetic flux through the loop), so the probability distribution of the level spacing should be that of the GOE ensemble of random matrices,

$$P(s) = \frac{\pi s}{2} e^{-\pi s^2/4}, \quad (5)$$

where s here is the level spacing in units of the mean level spacing at that energy. To compare to this prediction we first have to measure the density of states, which sets the mean level spacing. The average density of states $N(E)$ in each sector of total crystal momentum is shown in Fig. 1 for the case of chain length $L = 18$. Thus we obtain an energy-dependent mean level spacing $\Delta(E) = 1/N(E)$. The spacing of each pair of adjacent levels within one sector is divided by $\Delta(E)$ to yield the scaled level spacing s . The resulting probability distribution $P(s)$ for $L = 18$ is shown in Fig. 1, where we can see it agrees very well with the GOE form (5).

The Kubo formula (1) shows that a relevant statistical quantity that enters the conductivity at a given frequency ω is the mean-square value of the current matrix elements J_{mn} between energy eigenstates separated by an energy $\hbar\omega = |E_m - E_n|$. [Note that our eigenstates all have real amplitudes, so these matrix elements are all

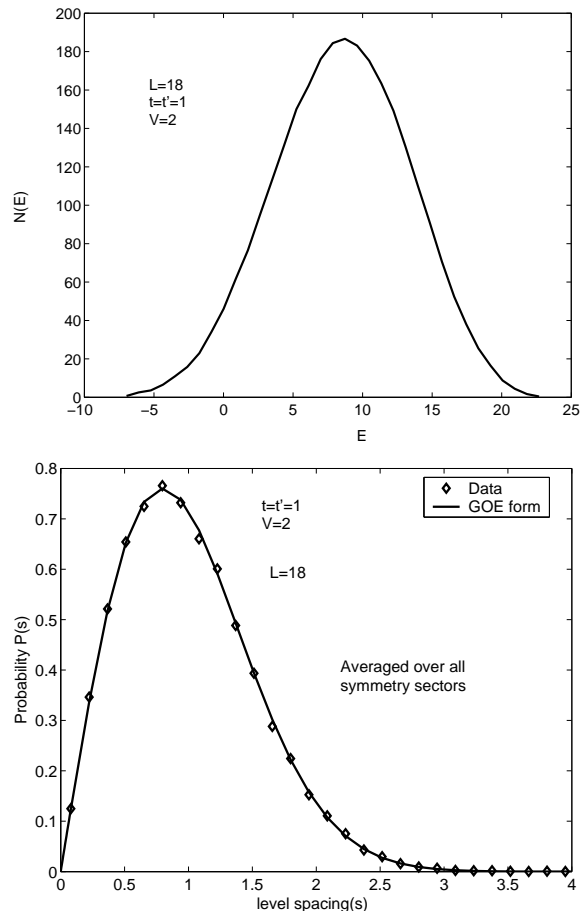


FIG. 1: (Top) The average density of states in each symmetry sector. (Bottom) The probability distribution of the scaled level spacing for the $L = 18$ system (data points) and the GOE form for this distribution (line), showing the excellent agreement.

real here.] Thus we were interested in characterizing the probability distribution of these current matrix elements. What we find is that the distribution is consistent with a Gaussian, with mean zero and a variance that depends on both the initial and final energies. The variance has a strong dependence on ω , giving $\sigma(\omega)$ its dependence on ω (see below). The variance also has a weaker dependence on the average energy $\bar{E} = (E_m + E_n)/2$. To examine the probability distribution of J_{mn} , we bin the matrix elements by both ω and \bar{E} , and look at all the J_{mn} 's that fall in one such bin of energies, accumulated over all total momentum sectors. We measure the first through fourth moments, M_1 through M_4 , of these distributions, observing that the odd moments are consistent with zero, and looking particularly at the ratio $R = M_4/M_2^2$ that is equal to 3 for the Gaussian distribution. If the bins are chosen too wide, the variance changes over the bin and the resulting distribution has a ratio R larger than 3. But as the bins are made narrower, R converges to 3, indicating that the current matrix elements do indeed

have Gaussian probability distributions. Since the variance depends much more strongly on ω than on \bar{E} , the bins are taken to be much narrower along the ω direction.

Thus we conclude that the total current operator, as written in the basis of the eigenstates of the Hamiltonian, is effectively a Gaussian random matrix that is, loosely speaking, “banded”, meaning the variance of the matrix elements J_{mn} depends smoothly on E_m and E_n . The “bands” of constant variance in this case do not run exactly parallel to the diagonal of the matrix. Of course, neither our Hamiltonian nor the current operator contain any random variables; the apparent randomness comes from the statistical properties of the highly excited eigenstates of our nonintegrable (and thus “quantum chaotic”) Hamiltonian. The total current operator, on the other hand, is integrable, with its eigenstates being the simultaneous eigenstates of all the single-particle momenta. When we write the Hamiltonian as a matrix in the basis of the eigenstates of the current operator, which is precisely what we do to diagonalize it numerically, it is a highly regular sparse matrix. [We have also looked at the *energy* current operator, which enters in the thermal conductivity and thermopower; the energy current operator is nonintegrable, and the Hamiltonian does look like a Gaussian random matrix when written in terms of the eigenstates of the total energy current.]

The final statistical characterization we have done is of the amplitudes $\langle n|\alpha\rangle$ when the eigenstates $|n\rangle$ of H are written in the basis of the eigenstates $|\alpha\rangle$ of J (and *vice versa*). These amplitudes, like the current matrix elements J_{mn} discussed above, appear to be mean-zero Gaussian random variables with a variance depending on two energies, namely E_n and the kinetic energy K_α of the current eigenstate. Each current eigenstate is also an eigenstate of the kinetic energy operator, which is the sum of the hopping terms in the Hamiltonian. As expected, a state $|n\rangle$ of high (low) total energy E_n consists primarily of states $|\alpha\rangle$ of high (low) kinetic energy K_α , but it appears to be quite uniformly and randomly extended over all the current eigenstates at each particular kinetic energy. Thus we find that both the eigenstates of H , and their current matrix elements appear to behave as Gaussian random variables with energy-dependent variances.

IV. THE CONDUCTIVITY

The conductivity is given by the Kubo formula (1). As remarked earlier, it is a series of delta functions for a finite-sized system, which can be binned to produce a smooth curve for $\sigma(\omega)$. Since the limit of zero frequency is of particular interest, we will focus much of our attention on low frequencies. Although the expression (1) does not apply at strictly zero frequency, it does contain a delta-function there that all levels contribute to. This zero-frequency feature has often been called (ambiguously) the “Drude peak”, and appears to have finite

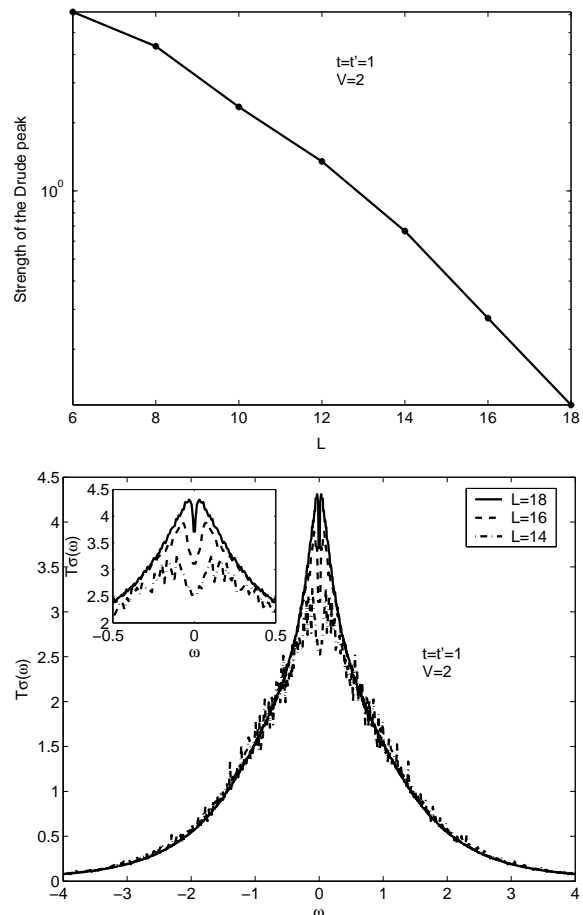


FIG. 2: (Top) Drude weight as a function of L . The Drude weight is expected to vanish exponentially with L . (Bottom) Conductivity as a function of frequency for $L = 18$, $L = 16$ and $L = 14$. The agreement among different system sizes is good at high frequencies but significant finite-size effects can be seen at low frequency. (Inset) Closer view of the low frequency regime. The dip in the conductivity around $\omega = 0$ is due to level repulsion. This dip rapidly narrows with increasing system size. The bins used here have a width equal to the mean level spacing at the maximum of the density of states for that L , except in the case of the main panel for $L = 14$, where the bins widths are instead chosen proportional to ω in order to reduce the scatter.

weight in the thermodynamic limit for integrable models. However, for nonintegrable quantum chaotic models such as we study here, the weight in this strictly elastic Drude peak vanishes strongly in the thermodynamic limit, see Fig. 2, top panel. This can be roughly understood by noting that the full conductivity (1), which has a finite large L limit, is a sum of $\sim e^{2sL}$ delta functions, where s here is the entropy density. Of these, only e^{sL} are at zero frequency (since there are no degeneracies within any symmetry sector). We find that the weight of the zero frequency terms in the sum are of the same order as those at small frequency, so the relative strength

of the so-called Drude peak at zero frequency drops as e^{-sL} with increasing L . A more careful analysis gives power-law in L prefactors to these exponential dependences. But the presentation on a semilog plot in Fig. 2 shows that our results are consistent with a Drude weight that vanishes exponentially with increasing L .

The conductivity is shown in Fig. 2 for our longer chains, of length 14, 16 and 18. To obtain fairly smooth functions, the delta functions are binned (see caption), and the elastic $\omega = 0$ “Drude” peak is left out of these plots. At high frequencies, the finite size effect is clearly very small, so these short chains give a good approximation to the thermodynamic limit. An interesting question that we do not yet have an answer for is: What is functional form of the conductivity at high frequencies (say, $\omega > t$), and what is the physics determining it? We find that $\sigma(\omega)$ appears to decrease faster than any power of ω in this regime.

While there appears to be good convergence to the thermodynamic limit of $\sigma(\omega)$ at high frequencies for these chain lengths, clear finite-size effects are seen at low frequencies. We find two sources of these finite-size effects: level repulsion, and diffusive “long-time tails”. The former is expected and has been discussed before in this and many other contexts, but the latter appears to be a new observation for this type of quantum many-body system. Level repulsion causes a reduction of $\sigma(\omega)$ at frequencies of order or less than the mean level spacing, because there are fewer pairs of levels with those energy differences that can produce the dissipation. The level spacing vanishes exponentially in the system size, so this feature, which appears as a dip in $\sigma(\omega)$ around zero frequency, narrows very rapidly with increasing L , as is apparent in the inset in Fig. 2.

Naively, one might expect (as we did when we started this project) that in this high temperature disordered regime with no long-range spatial correlations the conductivity of the infinite system would be a smooth analytic function of frequency in the vicinity of zero frequency. However, examination of our results in Fig. 2 show that this does not appear to be the case. The conductivity appears to have a sharp maximum at $\omega = 0$ that gets steadily sharper as L is increased. This sharp peak is apparent in published numerical data from other one-dimensional quantum models [5], but the reason for it appears not to have been discussed. As we show in the next section, long-wavelength diffusive modes of the energy and particle density generically interact nonlinearly to produce a nondivergent zero-frequency singularity of the form $\sigma(\omega) = a - b\sqrt{|\omega|} + \dots$ in these one-dimensional systems. In the top panel of Fig. 3 we show that our data appear to be consistent with such a form for the low-frequency conductivity in the large L limit. This behavior arises from a “long-time tail” in the autocorrelation function of the total current that decays with time difference as $\langle J(0)J(t) \rangle \sim t^{-3/2}$ at long times. We show in the bottom of Fig. 3 that our data for this autocorrelation for $L = 18$ do show such a power-law decay over a

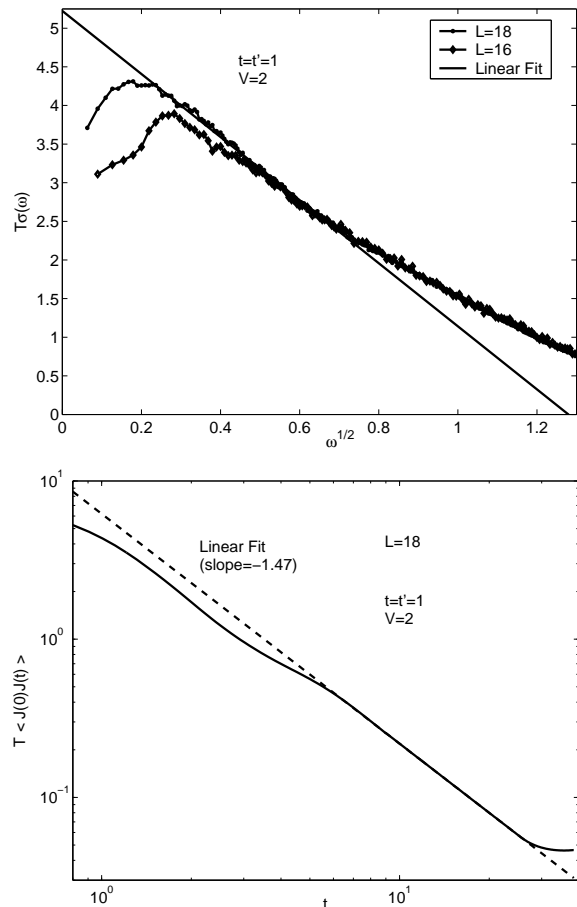


FIG. 3: (Top) Conductivity plotted versus $\sqrt{\omega}$ for $L = 16$ and $L = 18$. The straight line is a linear fit on this plot. The conductivity appears linear in $\sqrt{\omega}$ at low frequencies before it rounds off at very low frequency due to finite-size effects. The finite-size effects are, as expected, more pronounced for $L = 16$ than $L = 18$. (Bottom) Autocorrelation function of the total current vs. time on a log-log plot. There is a long-time tail with $\langle J(0)J(t) \rangle \sim t^{-3/2}$.

significant time range.

V. LONG-TIME TAILS DUE TO DIFFUSIVE MODES

Here we first give a more general argument inspired by our one-dimensional system. Consider an infinite many-body system in a disordered phase. If it has any conserved densities, such as energy, momentum, angular momentum, particle number etc., we may ask about the transport properties for these quantities. A long-wavelength disturbance in the conserved quantities relaxes at a (possibly complex) rate $\Gamma(\mathbf{q})$ where \mathbf{q} is the wavevector of the disturbance, and this rate is in general different for different linear combinations of the various conserved quantities. In the absence of long-range inter-

actions or propagating modes, the relaxation is diffusive: $\Gamma \sim Dq^2$ for small q . These long-wavelength diffusive modes in general produce singular behavior of the transport properties in the zero-frequency (long-time) limit, as discussed, for example, by Kirkpatrick, *et al.* [7]. This has been discussed in the context of fluids [8] where momentum conservation makes these effects quite strong, and in systems where quenched randomness appears to play an essential role [7].

For the Hamiltonian that we are studying, there are two conservation laws that give diffusive modes: energy and particle number. The lattice (*umklapp*) breaks the momentum conservation down to just the conservation of crystal momentum, which does not appear to produce any slow modes in the disordered phase.

To be a little more general, let us first consider a translationally- and rotationally-invariant system in a disordered phase with some number of conserved densities $n_\alpha(\mathbf{r}, t)$ in possibly more than one dimension. The conservation laws then dictate

$$\frac{\partial n_\alpha}{\partial t} = -\nabla \cdot \mathbf{j}_\alpha, \quad (6)$$

where $\mathbf{j}_\alpha(\mathbf{r}, t)$ is the current of conserved quantity α . Let us define the local densities n_α as the deviations from the average densities, so that our system has zero average densities $\langle n_\alpha \rangle = 0$. We assume the long-wavelength, low-frequency dynamics is diffusive, and expand the equilibrium coarse-grained dynamics in the densities and the wavevectors (spatial gradients). The currents are expanded as

$$\mathbf{j}_\alpha = -D_{\alpha\beta} \nabla n_\beta + E_{\alpha\beta\gamma} n_\beta \nabla n_\gamma + \dots + \eta_\alpha, \quad (7)$$

where D is the diffusivity matrix, η is noise (due to nonlinear couplings to short-wavelength modes) with an intensity given by a fluctuation-dissipation relation (e.g., [9]), and repeated subscripts are summed over. The lowest-order (in density and gradient) nonlinear correction to the diffusive behavior has also been shown explicitly; for example the term $E_{\alpha\beta\gamma}$ corresponds to the linear dependence of the local diffusivity matrix element $D_{\alpha\gamma}$ on the local density n_β .

What should be the low-frequency behavior of a transport coefficient like $\sigma(\omega)$? By the Kubo formula, this is given by the time Fourier transform of the autocorrelation function of the total (zero wavevector) current. Integrating the above expression, and thus leaving out any terms that are total derivatives, the total current is

$$\mathbf{J}_\alpha(t) = \int \mathbf{j}_\alpha d\mathbf{r} = \int \left[\frac{E_{\alpha\beta\gamma} - E_{\alpha\gamma\beta}}{4} (n_\beta \nabla n_\gamma - n_\gamma \nabla n_\beta) + \dots + \eta_\alpha \right] d\mathbf{r}. \quad (8)$$

Note that the total current is correlated with the densities only through the nonlinear corrections to simple diffusion; we will consider the generic case when these corrections are indeed nonzero. Through this nonlinearity, the zero-wavevector current is coupled to the slow, small-wavevector diffusive density modes; this is what produces

the long time tails. However, since the leading nonlinear coupling that we show explicitly here must be to an antisymmetric combination of the conserved densities, for a system with only one conserved density (and thus no antisymmetric combinations of densities), one has to go to significantly higher-order nonlinearities ($|\nabla n|^2 \nabla n$) to obtain the leading long-time tail in the current autocorrelations.

Writing the total current in terms of the long-wavelength density fluctuations in reciprocal space, we have

$$\mathbf{J}_\alpha = \frac{E_{\alpha\beta\gamma} - E_{\alpha\gamma\beta}}{2i} \int \mathbf{q} n_\beta(\mathbf{q}) n_\gamma(-\mathbf{q}) d\mathbf{q} + \dots + \eta_\alpha, \quad (9)$$

where $n_\beta(\mathbf{q})$ and $n_\gamma(\mathbf{q})$ are the spatial Fourier transforms of $n_\beta(\mathbf{r})$ and $n_\gamma(\mathbf{r})$. The low momentum fluctuations in $n_\beta(\mathbf{q})$ and $n_\gamma(\mathbf{q})$ decay diffusively. The eigenmodes of that decay are the linear combinations of the densities that diagonalize the diffusivity matrix. What we are doing here is considering the correction due to nonlinearity to the linear diffusive ‘‘fixed point’’ theory. These nonlinearities are irrelevant in a renormalization group approach, but give singular corrections to the leading diffusive behavior. The long-time tail we discuss here is one of those corrections. At this diffusive fixed point, in the basis of densities that diagonalizes the diffusivity matrix, the autocorrelations of the long-wavelength density fluctuations decay as

$$\langle n_\beta(\mathbf{q}, 0) n_\gamma(\mathbf{q}', t) \rangle \sim e^{-D_\beta q^2 t} \delta_{\beta\gamma} \delta(\mathbf{q} + \mathbf{q}') \quad (10)$$

for small q and large t , where D_β is the diffusivity for eigenmode β . Thus at long times, the autocorrelation of the total current behaves as

$$\begin{aligned} \langle J(0) J(t) \rangle &\sim \int d\mathbf{q} q^2 \exp(-Dq^2 t) + \dots \\ &\sim 1/t^{(d+1)/2} \end{aligned} \quad (11)$$

in d dimensions, where $D = D_\beta + D_\gamma$ is the sum of the two smallest diffusivities. Fourier transforming this to get the conductivity, we see that for one dimension and small ω , $\sigma(\omega) \sim a - b\sqrt{|\omega|} + \dots$; our numerical results (Fig.3) are quite consistent with this. In our finite-sized systems, the integrals on q are replaced by sums, which has the effect of rounding out this singularity at a frequency of order D/L^2 . This rounding is apparent in Fig. 3, and it can be seen to be reduced with increasing L . Note that the characteristic frequency of this diffusive finite-size effect vanishes only as L^{-2} with increasing size, in contrast to the scale for the level repulsion, which vanishes exponentially in L .

This explanation of the long-time tail in the autocorrelation of the total current makes certain assumptions and predictions about the dynamics and correlations of the long wavelength modes, which we have checked numerically within our model. First, it assumes that the dynamics of the long-wavelength fluctuations in the particle density n and the energy density e are diffusive. We

have checked this by calculating their dynamic correlations: $\langle |n(q, \omega)|^2 \rangle$, $\langle |e(q, \omega)|^2 \rangle$, and $\langle n(q, \omega)e(-q, -\omega) \rangle$ for the chain of length $L = 18$. At small q and ω these fit quite well to the expected diffusive behavior. The two diffusivities differ by approximately a factor of two. The faster eigenmode of the diffusion has a larger component of particle density than energy density, and *vice versa* for the slower mode.

Another assumption is that the long-wavelength modes interact nonlinearly to contribute to the total (zero momentum) current, as given by Eq. 10 above. For our finite-size 1d system with discrete momenta and just the two densities, n and e , this may be rewritten for the particle current as

$$J = C \sum_{q>0} i(\sin q)(n(q)e(-q) - n(-q)e(q)) + \dots + \eta, \quad (12)$$

where C is the nonlinear coupling. Thus we have measured C to check that it is indeed nonzero. To do this, we define the nonlinear combination of the densities at momentum q :

$$N(q) = i(\sin q)(n(q)e(-q) - n(-q)e(q)), \quad (13)$$

and measure its correlations with itself $\langle N(q)N(q') \rangle$ and with the current. We find that the correlations between N 's at different q 's are quite small compared to the variances $\langle N^2(q) \rangle$. To get estimates of the coupling C , we thus note that

$$\langle N(q)J \rangle \cong C \langle N^2(q) \rangle; \quad (14)$$

this gives us an estimate of C for each q , and we find that these estimates agree well with one another at small q and are indeed nonzero, as expected.

The specific form of the long-time tails that we derive above are for the case of relaxational dynamics and short-range interactions, where the conserved densities relax diffusively. Of course, charge carriers in real materials interact via the long-range Coulomb interaction, and the long-wavelength mode corresponding to the charge density, the plasmon, does not show diffusive relaxation; it is likely overdamped at high T , relaxing at a nonzero rate. Thus conserved energy and charge are not alone sufficient to produce the long-time tails discussed above once

Coulomb interactions (or other sufficiently long-range interactions) are included. What is needed is at least two conserved densities that relax diffusively. One possibility is ionic conductors, where there are multiple conserved charge carriers that can combine to produce another neutral, diffusively-relaxing hydrodynamic mode in addition to the energy.

VI. CONCLUSIONS

We have studied the frequency-dependent conductivity of a non-integrable fermionic chain with short range interactions. Our studies show that such a system can be regarded as quantum chaotic in the sense of random matrix theory, as can the current matrix elements that go into the Kubo formula for the conductivity. We have confirmed that charge transport in this system is not ballistic but diffusive with non-linearities. These non-linearities give rise to a non-analytic behavior for the optical conductivity at low frequencies which we understand through hydrodynamic arguments. We observe that the system shows finite-size effects at low frequency arising from Wigner-Dyson level repulsion and from the low momentum fluctuations of the conserved quantities in the Hamiltonian.

The methods used to obtain these results are readily generalizable to further explorations of the finite temperature behavior. The list of open questions includes other dynamic response functions and transport coefficients (e.g. Peltier and heat conductivities), an extension to two dimensions, a systematic investigation of the high temperature series for transport, whose first term for the conductivity has been computed here, and an extension to long range interactions. We shall report on some of these in the near future.

Acknowledgments

We are grateful to A. Lamacraft, J. Lebowitz, S. Kivelson and S. Sondhi for illuminating discussions. The authors would also like to thank the NSF for support through MRSEC grant DMR-0213706.

-
- [1] Y. Y. Wang, N. S. Rogado, R. J. Cava and N. P. Ong, Nature 423, 425 (2003); cond-mat/0305455.
 [2] E.g., Y. Ando, G. S. Boebinger, A. Passner, N. L. Wang, C. Geibel, and F. Steglich, Phys. Rev. Lett. **77**, 2065 (1996); Y. Ando, A. N. Lavrov, S. Komiyama, K. Segawa, and X. F. Sun, Phys. Rev. Lett. **87**, 017001 (2001); Y. Wang, N. P. Ong, Z. A. Xu, T. Kakeshita, S. Uchida, D. A. Bonn, R. Liang, and W. N. Hardy, Phys. Rev. Lett. **88**, 257003 (2002); for broader perspective see also P. W. Anderson and C. C. Yu, *Proc. Int. School of Physics Enrico*

- Fermi* (Edited by F. Bassani, F. Fumi and M. P. Tosi), North-Holland, Amsterdam (1985) p. 767; V. J. Emery and S. A. Kivelson, Phys. Rev. Lett. **74**, 3253 (1995); S. B. Arnason, S. P. Herschfield, and A. F. Hebard, Phys. Rev. Lett. **81**, 3936, (1998); O. Gunnarsson, M. Calandra, and J. E. Han, Rev. Mod. Phys. **75**, 1085 (2003) and references therein.
 [3] I. Peschel, *et al.*, editor, *Density Matrix Renormalization: A New Numerical Method in Physics*, Springer Verlag, 1999; H. G. Evertz. Adv. Phys., **52**, 1 (2003); V. E. Ko-

- repin, N. M. Bogoliubov, and A. G. Izergin, *Quantum Inverse Scattering Method and Correlation Functions*, Cambridge Univ. Press, 1993.
- [4] A. A. Abrikosov, L. P. Gorkov, I. E. Dzyaloshinski, *Methods of quantum field theory in statistical physics*, Dover Publications, 1975.
- [5] X. Zotos, Phys. Rev. Lett. **92**, 067202 (2004); X. Zotos and P. Prelovsek, cond-mat/0304630; F. Heidrich-Meissner, A. Honecker, D. C. Cabra, and W. Brenig, cond-mat/0406378.
- [6] D. A. Rabson, B. A. Narozhny, and A. J. Millis, Phys. Rev. B **69**, 054403 (2004).
- [7] T. R. Kirkpatrick, D. Belitz, and J. V. Sengers, J. Stat. Phys. **109**, 373 (2002).
- [8] J. R. Dorfmann and E. G. D. Cohen, Phys. Rev. Lett. **25**, 1254 (1970).
- [9] P. C. Hohenberg and B. I. Halperin, Rev. Mod. Phys. **49**, 435 (1977).